

7. PERMEABILITY, UNDERPRESSURES, AND CONVECTION IN THE OCEANIC CRUST AT DEEP SEA DRILLING PROJECT HOLE 504B¹

Mark D. Zoback, United States Geological Survey, Menlo Park, California
and

Roger N. Anderson, Lamont-Doherty Geological Observatory and Department of Geological Sciences,
Columbia University, Palisades, New York

ABSTRACT

In order to study the variation in physical parameters responsible for the transition from convective to conductive heat flow near mid-ocean ridges, *in situ* permeability and pore-pressure measurements were made 200 meters into oceanic crustal Layer 2A in DSDP Hole 504B, on the south flank of the Costa Rica Rift. Conventional "slug" and constant-rate injection tests were made below a hydraulic packer set at various depths in the hole. The packer was first set in a massive flow unit 37 meters below the sediment/basement interface. The bulk permeability of the 172.5 meters of pillow basalts and basaltic flows below the packer was found to be about 40 millidarcys (4×10^{-10} cm²). Measurements over 3- and 15-meter intervals at the bottom of the hole in an altered pillow zone indicated a bulk permeability of 2 to 4 millidarcys and formation pore pressures approximately 10 bars (~2%) below hydrostatic. Interpretation of the data with respect to simple numerical convection models suggests that the transition from convective to conductive heat flow is controlled by the cessation of convective heat transport through the sedimentary layer, rather than the cessation of convection in the basement. Furthermore, the agreement between observed and modelled underpressures implies that Hole 504B penetrated an active ocean crustal convection system. The thick sedimentary layer, layers of basal chert, and massive flow basalts above the Layer 2A pillow flows apparently form an impermeable lid, effectively isolating the convective system from the ocean.

THE PROBLEM

Convection of sea water through the oceanic crust at mid-ocean-ridge axes is now a well-established physical observation. Hydrothermal plumes exhaling metal-saturated "black smoke" at temperatures of 350°C and velocities of meters per second have been captured dramatically on film and video tape (Spiess et al., 1980). Mantle-outgassing anomalies (Clarke et al., 1970; Lupton et al., 1980) and large fluxes of major, minor, and trace elements out of the ridge axis (Corliss et al., 1979; Edmond et al., 1979) also indicate intense hydrothermal activity. Such activity was first observed at the Galapagos Spreading Center, where a remarkable suite of animal life including giant tube worms and large clams were found to be subsisting on sulfide-oxidizing bacteria near the hot springs (Corliss et al., 1979).

Mid-ocean-ridge-axis geothermal systems appear to evolve to colder-water convection systems which are active to great distances on the flanks of the ridges. The largest set of observations arguing for this continued convective activity is geothermal measurements. Regionally, much of the predicted heat flux of the cooling lithosphere is found to be missing when observations of conductive heat loss at the sea floor are made (Anderson and Hobart, 1976; Sclater et al., 1976; Anderson et al., 1977). Heat is still missing when the component of heat loss due to convection of pore water through the sur-

ficial sediments is added to this conductive component. The combined flux increasingly approximates that expected from lithospheric plate models as age of the oceanic crust and the thickness of the sedimentary blanket increase (Anderson et al., 1979). Interpretations of ridge-flank heat-flow data and thermal models of cooling oceanic lithosphere suggest that away from the axes all mid-ocean ridges show a transition from predominantly convective to conductive heat loss at the sea floor. The age at which the cessation of convective heat loss occurs varies from ocean to ocean. It occurs beyond 80 m.y. in the Atlantic, 60 m.y. in the Indian, and 20 m.y. in the Pacific (Anderson et al., 1977). The Galapagos Spreading Center exhibits the most rapid transition from convective to conductive heat loss. Beyond 5-m.y.-old sea floor, on the flank of this spreading center, the surficial thermal regime is predominantly conductive. The locale which displays this transition most clearly is the Costa Rica Rift, the easternmost segment of the Galapagos Spreading Center (Fig. 1) (Anderson and Hobart, 1976). A geothermal profile away from the spreading axis shows the typical though paradoxical increase in observed heat flow with increasing age and sediment thickness on the southern flank of the Costa Rica Rift (Fig. 1; Langseth et al., this volume).

In the study reported here, we set out to measure the physical parameters which might directly control the transition from convective to conductive heat transfer across the sea floor on the flanks of Costa Rica Rift in 5.9-m.y.-old crust (Fig. 1). The basic question we wish to address is whether the heat flow transition is due to the cessation of convective heat transfer through the

¹ Cann, J. R., Langseth, M. G., Honnorez, J., Von Herzen, R. P., White, S. M., et al., *Init. Repts. DSDP, 69*: Washington (U.S. Govt. Printing Office).

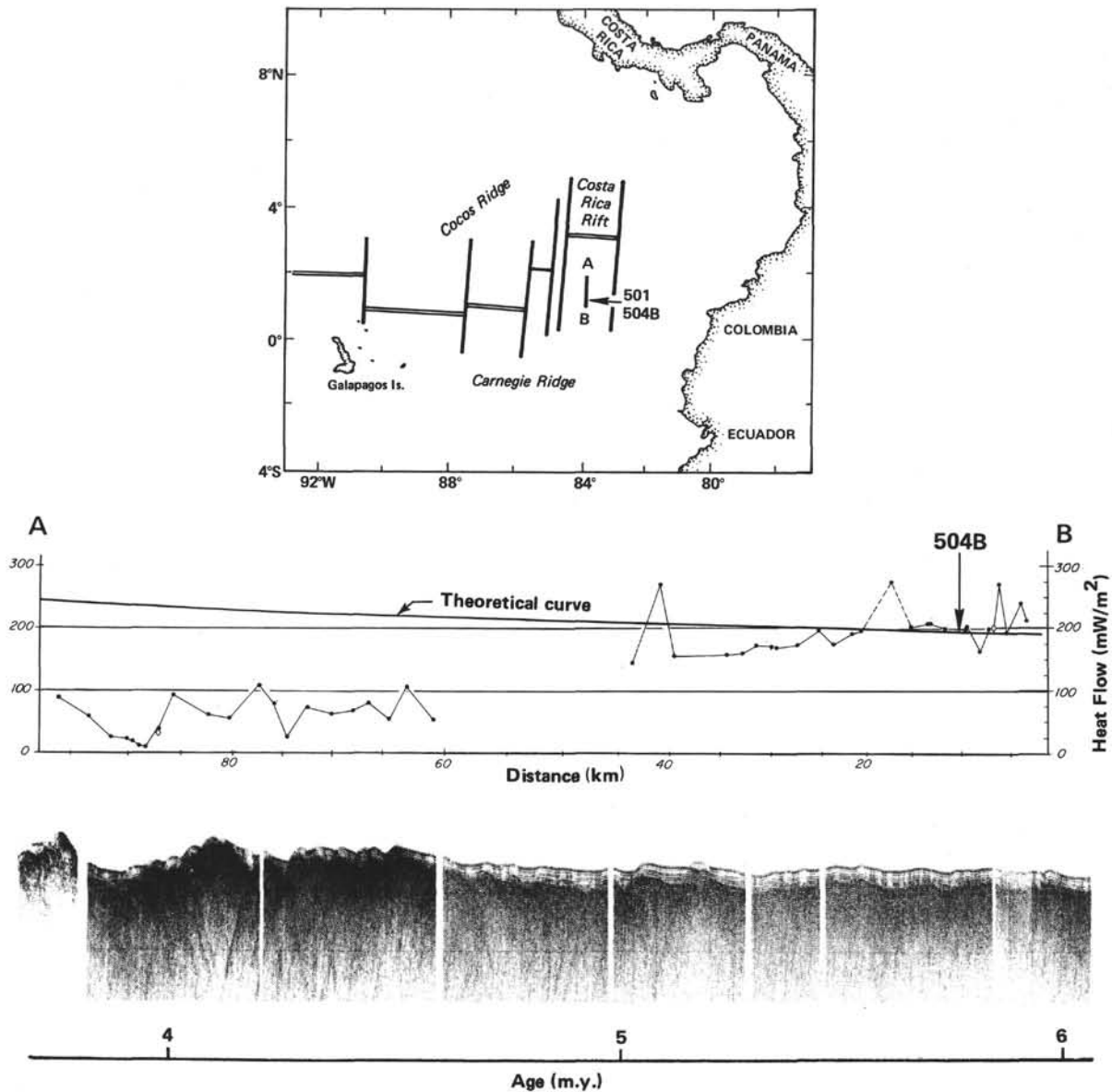


Figure 1. Heat flow (dots) versus age on the south flank of the Costa Rica Rift (index map), shown over the seismic-reflection profile, showing increase in sediment thickness with age on the ridge flank. Locations of DSDP Holes 501 and 504B are indicated.

sedimentary layer and/or to a cessation of convection in the basement (perhaps due to the progressively increasing alteration and remineralization of the older crust).

THE WORKING MODEL

Near the Galapagos Spreading Center, non-linear thermal gradients, widespread pore-water chemical anomalies, and metallogenesis show that a convection system penetrates the sedimentary layer and therefore carries significant heat directly from the oceanic crust to the oceans (Green et al., 1981). However, as the sea floor spreads away from the ridge axis, the convective component of heat transfer is gradually replaced by a totally conductive thermal regime at the sea floor.

To develop insight into how the heat-flow transition is dependent upon measurable physical properties, An-

derson and Skilbeck (in press) modeled the oceanic crust and overlying sediment as a two-layer porous medium. In this model, cellular convection is driven with a horizontally varying, sinusoidal pressure field of arbitrary amplitude. Parameterization of the sealing mechanism suggests that significant transport of heat by convection stops across the sea floor if the permeability of the sediment (k_s) divided by the sediment thickness (h) is much less than the wave number (a) (defined as π /half-wavelength) of each cell times the oceanic crustal permeability (k_b). Gartling (1981) constructed a finite-element model of this two-layer porous media example, and further quantified the relationship to show that whenever

$$\frac{k_s}{ahk_b} < 0.1 \tag{1}$$

convection becomes an insignificant carrier of heat across the top of the sedimentary layer. Our working model, then, is the hypothesis that the transition from convective to conductive heat flow is due to the cessation of convection through the sedimentary layer, and that this can be analyzed by studying variations in the physical parameters of Equation (1). Thus, if k_s is sufficiently small, or ahk_b is sufficiently large, convective heat transport through the sediments essentially stops. It should be emphasized that when Equation (1) is satisfied, convection may continue to be vigorous in the basement layer beneath the sediment (the sediment would then form a hydraulic lid). However, if the basaltic permeability decreased to too small a value for the Rayleigh number of the system to remain above critical, basement convection would stop, independent of the interrelation between sedimentary and basaltic properties defined in Equation (1), and a transition from convective to conductive heat flow would also result.

In order to test these concepts, it is necessary to know sediment and crustal permeabilities, sediment thickness, and the wavelength of the heat-flow variation along the sea floor. Although measurements of wavelength (e.g., Anderson et al., 1979; Davis et al., 1980) and sediment thickness are relatively easy, and sediment-permeability data have been accumulating rapidly in the last few years (e.g., Bryant et al., 1975; Abbott et al., 1981; Crowe and Silva, 1981), no direct observation of the permeability of the oceanic crust had been made prior to this study. Indirect predictions of the permeability of oceanic crustal rocks have varied enormously. Crack width-to-spacing ratios, formation electrical resistivity, and porosity data have yielded values higher than most natural geological formations on land: 10^2 to 10^4 darcys (10^{-4} to 10^{-6} cm²) (Salisbury et al., 1979; Johnson, 1980a). Geothermal convection models (Lister, 1972; Anderson et al., 1977) have suggested values similar to good oil-producing sandstones, 1 to 1000 millidarcys (10^{-11} to 10^{-8} cm²). Values for altered to fresh, unfractured basalt ranging from 0.001 to 1 microdarcys (10^{-14} to 10^{-17} cm²) were measured in the laboratory (Johnson, 1980b). Seldom in geology have different physical considerations of the same phenomenon made such disparate predictions: a range of some ten orders of magnitude for the permeability of the ocean crust.

Because an understanding of oceanic crustal permeability is so crucial to understanding convection beneath the sea floor, we made the first *in situ* measurements of permeability in Layer 2A of the oceanic crust by conducting flow tests across packed intervals at DSDP Hole 504B from the D/V *Glomar Challenger* (Leg 69). Such *in situ* estimates are considerably more reliable than results obtained from laboratory measurements of cores, or from estimates based upon counting cracks in the cores. The high-heat-flow flank of the Costa Rica Rift was chosen because of the apparent rapid sealing of convection and expected good drilling conditions close to the ridge axis.

THE EXPERIMENTS

Three types of hydrogeologic experiments were conducted in Hole 504B. In order to determine *in situ* per-

meability and pore pressure, a packer was inflated down-hole, isolating varying segments of hole. In one type of test, a pressure pulse or "slug" was pumped into the formation, using surface pumps. The decay character of these pressure pulses was measured, and permeability was determined. The method is described in detail below. Because fractured media are not uniformly permeable, a "bulk" permeability over the tested interval is computed. Experiments conducted over a number of different intervals yield the variation in permeability in different lithologic units. Because the formation turned out to be rather permeable, a constant-rate injection test was also conducted. In this case, the surface pumps maintain a constant flow rate down-hole for several tens of minutes, and the formation pressure is monitored. This test also yields a value for bulk permeability.

The second type of experiment that was done was to estimate formation pore pressure. We were able to do this in two ways. In a permeable interval, we compared the pressure within the packed-off interval before and after flow tests were conducted. In the less-permeable intervals, we analyzed the slug tests, because as the pressure pulses decay, they asymptotically approach *in situ* pore pressure.

The final type of experiment was designed to study *in situ* fractures and voids. An ultrasonic bore-hole televiewer (described by Zemenek et al., 1970) was deployed down-hole to give an "acoustic" picture of the natural fracture distribution of the upper oceanic crust and to help us interpret our permeability results in terms of lithostratigraphic variations. The results of the televiewer survey are summarized below and described in detail by Anderson and Zoback (this volume).

The Packer

A Lynes International during-drilling safety test tool (DDST) was included in the bottom-hole assembly during the first re-entry of Hole 504B after drilling was completed. The DDST tool consists of a 1-meter long inflatable rubber packer mounted 3 meters above the drill bit. The packer was inflated by dropping a "go-devil" down the pipe. Two kinds of go-devils were used (illustrated in the insets of Fig. 2). For the permeability and pore pressure tests, a "safety" go-devil diverts fluid flow into the packer until inflation produces a firm seal against the hole. A shear plug is then blown, which opens the packed formation to direct pumping from the surface (Fig. 2B). As flow through the annulus (the space between the wall of the hole and the outside of the drill pipe) is prevented by the inflated packer, the fluid must flow directly into the formation below the packer. The packer remains locked in the inflation mode until a steel ball is dropped to deflate the tool. A down-hole pressure recorder is mounted at the front tip of the go-devil, giving direct *in situ* pressure measurements in the packed-off formation. In the other type of test, a "sampler" go-devil is used, and a 60-liter sample of pore fluid is automatically taken after the packer inflates (Fig. 2C). In this case, the sample chamber and the hole beneath the packer are in communication, and the pressure recorder again gives *in situ* formation pressure during the sampling operation.

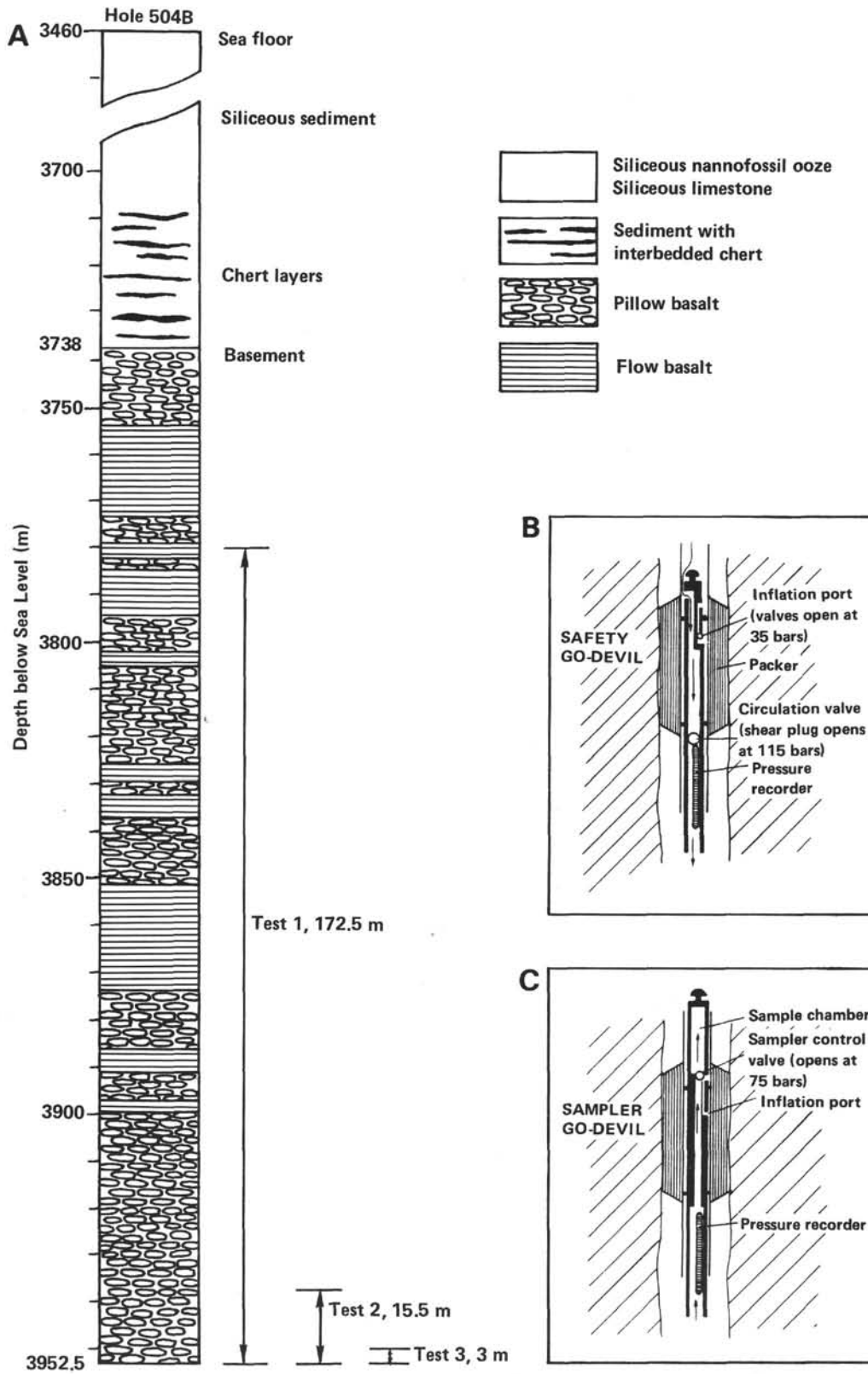


Figure 2. A. Lithostratigraphy from bore-hole televiwer records in DSDP Hole 504B (Anderson and Zoback, in press); test intervals of Figure 3 and 4 outlined. Line drawings illustrate safety (B) and sampler (C) go-devil operations.

The Bore-Hole Televiwer

In order to map the natural fracture distribution of the hole and also to examine the lithostratigraphy of the entire hole (only 29% of the formations drilled were recovered during the coring operation), an ultrasonic bore-hole televiwer was deployed down-hole in Hole 504B and also in Hole 501 (just 1 km west of 504B). The variations in lithologies encountered down-hole are important to our understanding of the permeability and pore-pressure measurements described below. The general lithostratigraphy of Hole 504B is shown in Figure 2A. At Hole 504B, the water depth is 3460 meters. Drilling during Leg 69 penetrated 274.5 meters of siliceous nanofossil ooze, siliceous limestone, and chert, and 214 meters of basaltic pillows and flows, to a total depth of 3952.5 meters below sea level (Fig. 2A). A series of dense chert layers was encountered 30 meters above basement in both Holes 501 and 504B. These layers were followed by thin chert lenses to the basement/sediment contact. A thick basaltic flow ranging in thickness from 7 meters at Hole 501 to 10 meters at Hole 504B was encountered below 10 meters of large-diameter pillow basalts (10–100 cm). Below 50 meters of alternating thin pillows and thick flow units, the basement grades into well-cemented, smectite-rich, small-diameter (~10 cm) pillows at the bottom of the portion of Hole 504B drilled during Leg 69 (CRRUST, in press).

The Constant-Rate Injection Test

The packer was initially set at 3780 meters, in a flow unit 172.5 meters above the bottom of the hole (Fig. 2A) at the end of Leg 69 drilling (214 m below the sediments). Initial slug tests showed the formation to be too permeable for this measurement technique (because the pulses decayed too rapidly to be analyzed) (test 1; Fig. 3), so a constant-rate injection test was conducted. For 20 minutes, the *Challenger* rig pumps flowed 100 gal/min of surface sea water down-hole and into the formation. The pressure rose quickly to 13.2 bars above hydrostatic and remained within ± 0.3 bars of that value for the final 18 minutes of the test, indicating that steady-state conditions had been achieved. Glover's formula (Snow, 1968) for constant-rate injection tests gives formation permeability (k).

$$k = \frac{cQ \ln[2L/D]}{\pi 2LH} \quad (2)$$

where

- Q = quantity of water pumped per unit time;
- L = length of packed interval;
- D = hole diameter;
- H = net head acting on the formation;
- c = $\mu/g\rho$ where μ is the fluid viscosity, g is the acceleration due to gravity, and ρ is fluid density; this term converts from hydraulic conductivity (with units of cm/s) to permeability (with units of cm² or darcys).

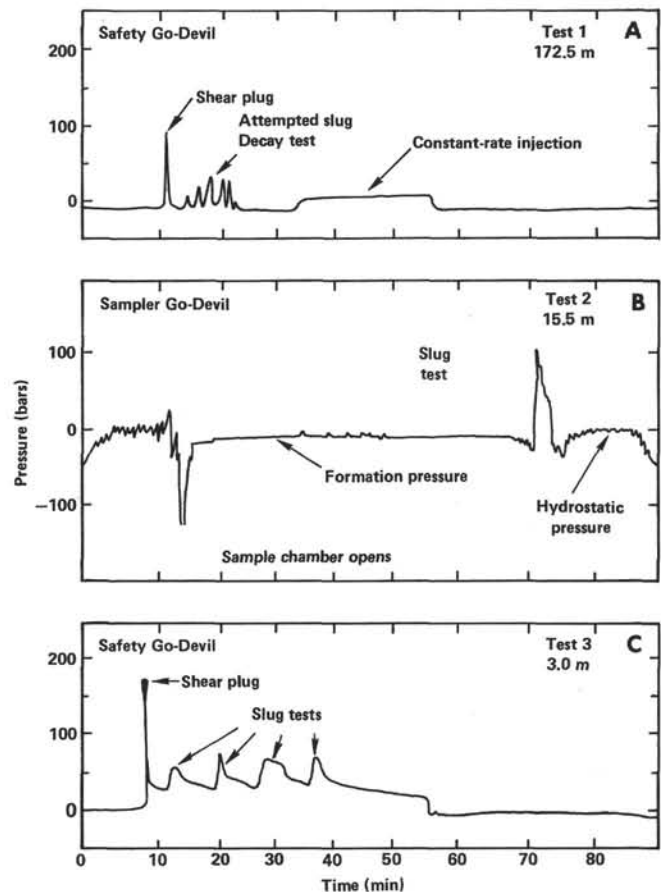


Figure 3. *In situ* pressure versus time for three hydraulic tests made below the packer at different depths in the hole (see text).

For test 1 (the 172.5-m test interval), the bulk permeability computed from (2) is 37 millidarcys, or 3.7×10^{-10} cm².

The Slug Tests

Moving down-hole, a slug test was conducted over the bottom 15.5 meters of the hole. This was a fortuitous test which was made possible when the regulator valve on the sampler go-devil failed, instantly opening the 60-liter evacuated chamber directly to the formation. Due to the sudden low pressure beneath the rubber packer element, it was violently drawn down and over the drill collar, balling-up against the well bore between the packer and the core bit. The formation was not only packed-off 15.5 meters off-bottom (good news) but the drill string was stuck to a pull of 400,000 lbs (bad news). During the course of trying to free the drill string, a slug test was conducted (test 2, Fig. 3). This slug test resulted in a normalized pressure-versus-time plot, from which permeability was computed in the following manner (after Bredehoeft and Papadopoulos, 1980).

Consider a well system which is suddenly pressurized by injecting an additional amount of water above the static level with a high pressure pump. The system is then shut in, and the head decay (H) following the pressure pulse (H_0) is monitored. It is assumed that flow in-

to the tested interval is primarily radial, and that the hydraulic properties of the formation remain constant throughout the test. Another assumption is that volumetric changes due to the expansion and contraction of components of the system other than the fluid are negligible. The pressure decay (H/H_0) is shown by Cooper et al. (1967) and Bredehoeft and Papadopolus (1980) to be a function of two parameters, α and β , defined as

$$\alpha = \frac{\pi r^2 S}{V_w C_w \rho_w g} \quad \beta = \frac{\pi T t}{V_w C_w \rho_w g} \quad (3)$$

where

- S = storage coefficient of the tested interval;
- V_w = volume of system;
- C_w = compressibility of water;
- ρ_w = density of water;
- γ = gravitational acceleration;
- t = time.

Cooper et al. (1967) and Bredehoeft and Papadopolus (1980) present a complex formulation for the pressure-decay function that has been tabulated into a set of type curves in which the shapes of different decay curves for varying α 's are shown as a function of H/H_0 and β (Fig. 4A). Permeability (k) is determined from the transmissivity, T , by

$$k = \frac{Tc}{b} \quad (4)$$

where b is the thickness of the interval isolated by the packer, and c again is introduced to convert from hydraulic conductivity to permeability, as in Equation (2).

A semilogarithmic plot of H/H_0 versus time is superimposed on the type-curves and translated along the β axis into a position to best fit one of the curves. The time, t^* , is read off at the point where the slug-test data overlies the $\beta = 1$ point on the type curve for appropriate α . Then, from (3) and (4),

$$k = \frac{V_w C_w \rho_w g}{b \pi t^*} \quad (5)$$

The comparison of the shape of the H/H_0 -versus-time curve to the type-curve also gives a test of the success of the experiment. If the shape of the slug-test curve differs significantly from that of the type curve, something went wrong with the experiment. Pressure-decay curves from experiments in which substantial leakage occurs around a damaged packer result in curve shapes dramatically different from those of the slug test.

The data from test 2 (Figs. 3B and 4B), the 15.5-meter slug test, fit $\alpha = 10^{-1}$ very satisfactorily, and Equation (5) gives $k = 4.5$ millidarcys ($4.5 \times 10^{-11} \text{ cm}^{-2}$). For the test conducted over the lowermost 3 meters of the hole (211–214 m below the sediments; Figs. 3C and 4C, pulse 1) the best-fitting type curve is $\alpha = 10^{-1}$, and $k = 3.2$ millidarcys ($3.2 \times 10^{-11} \text{ cm}^2$).

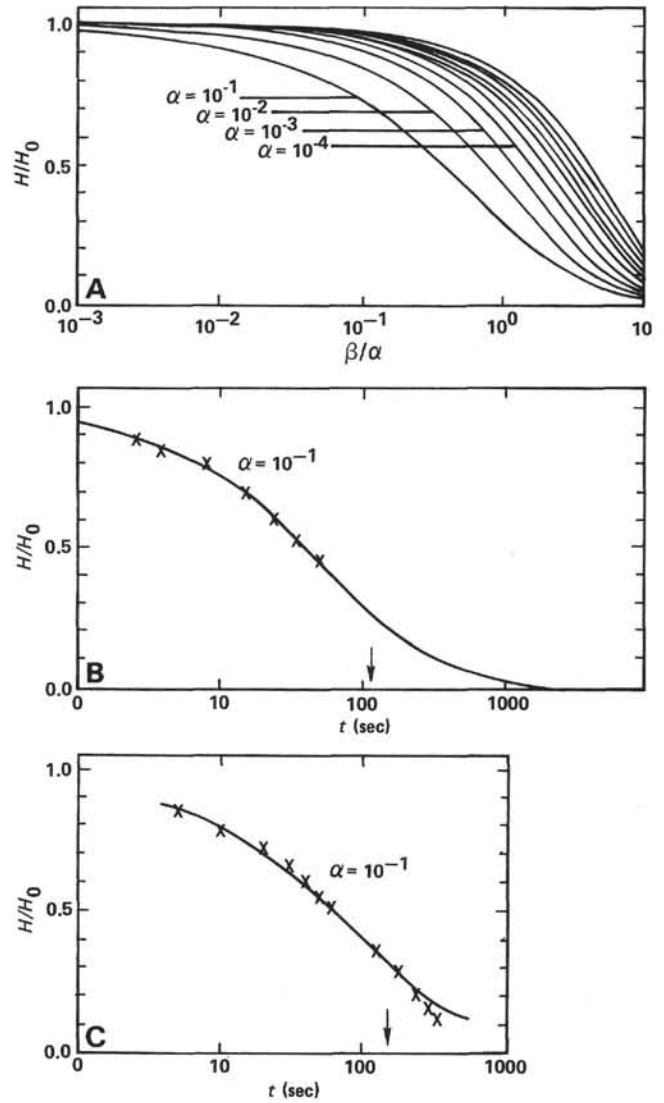


Figure 4. A. Slug-test theoretical curves from Bredehoeft and Papadopolus (1980) and Cooper et al. (1967). The decay in pressure H versus the initial pulse H_0 is plotted versus β for various α 's (Eq. 3, test). B. Slug tests over 15.5 meters at bottom of hole. C. Slug test over 3 meters at bottom of hole.

Formation Pore Pressure

A measure of the formation pore pressure first was obtained when the packer was stuck 15.5 meters off the bottom of the hole during test 2, because when the sampler go-devil was used the down-hole pressure gauge recorded the formation pressure, not the hydrostatic pressure. The pressure gauge monitored a constant pressure of 8 ± 0.1 bars below hydrostatic pressure for more than 1 hour after the chamber opened, but before the hydraulic seal to the hole was broken, and hydrostatic head again was observed (Fig. 3, test 2). In other words, the *in situ* pore pressure near the hole was about 2% below the hydrostatic pressure of the water column (~ 400 bars).

It is also possible to estimate the *in situ* pore pressure from the long-term pressure resulting from the decay of

the slug tests (Fig. 3, test 3). Cooper et al. (1967) have shown that for $\alpha = 10^{-1}$ (which is appropriate to our tests; Fig. 4) and $H/H_0 \leq 0.5$, the decay of the pressure with time approximates that predicted by the line source of Ferris and Knowles (1954). That is, H/H_0 is decaying in a manner inversely proportional to time, and slowly approaching the *in situ* pore pressure. Because the line-source approximation is applicable when $H/H_0 \leq 0.5$, it is possible to use a standard extrapolation technique to determine the pore pressure (Matthews and Russell, 1967, pp. 18–19). They show that

$$H = H^* - \frac{q\mu}{4\pi kh} \ln \left[\frac{t + \Delta t}{\Delta t} \right] \quad (6)$$

where H^* is the *in situ* pore pressure, Δt is the shut-in time, t is the time during which flow into the interval occurred, prior to the test, and q is the average flow rate during t . By plotting H as a function of $t + \Delta t/\Delta t$ on a logarithmic scale, we can determine H^* by linear extrapolation of H to $t + \Delta t/\Delta t = 1$ (i.e., to $\Delta t \rightarrow \infty$).

For these experiments, t is taken as 30 hours, the time between the completion of drilling, attachments of the packer assembly, and “tripping” into the hole to conduct the test. The four slug tests with the packer set 3 meters above the bottom of the hole (test 3, Fig. 3C) all extrapolate very clearly to negative pore pressures. The longest test shows an *in situ* pore pressure of about -12 bars (Fig. 5). Note that from Equation (6) the test results should not be linear on a semilogarithmic plot, but should converge as Δt passes the time at which $H/H_0 = 0.5$. Although an extrapolation technique such as this is imprecise, the results are reasonably consistent with the value of -8 bars indicated by test 2.

DISCUSSION

The data presented above indicate that (1) sections of Layer 2A of the oceanic crust on the flank of the Costa Rica Rift have less than hydrostatic pore pressure, and (2) that the basalt is fairly permeable (~ 37 millidarcys

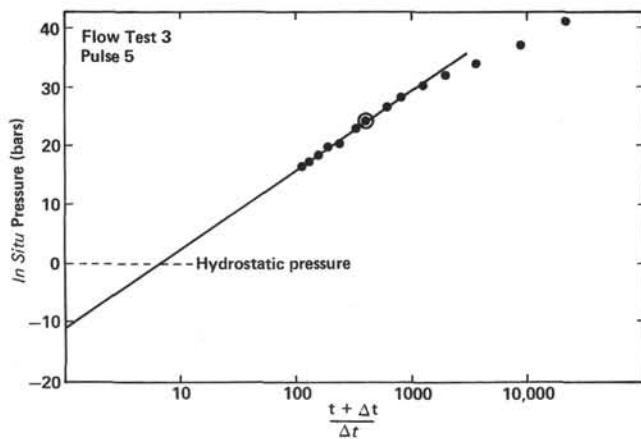


Figure 5. Extrapolation of slug-test pressure-decay curve from last (and longest) pulse (Fig. 3C) to *in situ* pore pressure. H/H_0 decays linearly after time at which $H/H_0 = 0.5$ (circled dot).

in the pillow basalts of the lower 172.5 meters of the hole, and 2 to 4 millidarcys in the cemented pillows at the bottom of the hole). The down-hole temperature logging results of Becker et al. (this volume) also indicate that the hole penetrated an underpressured zone, because depressed down-hole temperatures (indicating downward flow of sea water into the formation) were measured in the lower part of the hole 54 days after the completion of drilling. They calculated that the rate of downward flow into the crust was about 30 gallons per minute, and that most of the flow passed into the formation through a zone 50 meters below the large basaltic sill in which we set our packer for the 172.5-meter slug test. From our measurement of the negative pore pressure responsible for this down-flow, they calculated a permeability value of about 200 millidarcys, which is higher by a factor of five than our constant-rate injection test result of 37 millidarcys over a considerably larger interval.

These observations have important implications regarding hydrothermal processes near the Costa Rica Rift. The coexistence of underpressures and high-permeability basalt suggests that cellular convection might be active in Layer 2A, and that Hole 504B penetrated into such a cell. However, the agreement between the average heat flow measured at the sea floor and that predicted by conductive-lithospheric-cooling models implies that any convection in the basement is sealed below the sea floor (Fig. 1B). Do our measurements then quantitatively support the existence of a capped convection system on the flank of the Costa Rica Rift?

Let us return to the Anderson-Skilbeck-Gartling model for convection in a basaltic layer possibly sealed by a relatively impermeable sedimentary lid. The model requires that the hydraulic admittance of the sedimentary layer (k_s/h) be less than one-tenth that of the basaltic layer (ak_b), and that the Rayleigh number, R , of the basaltic system be above the critical Rayleigh number, R_c . If convection is occurring, the areal variability of the surface heat flow in the area (± 25 mWm $^{-2}$, about the mean of 200 mWm $^{-2}$, as shown by Becker et al., this volume) suggests a cell dimension of about 5 km. The wave number, a , is then 6.3×10^{-4} m $^{-1}$.

Abbott et al. (1981) have measured *in situ* and laboratory permeability of sediments similar to those at the surface near Hole 504B of about 5 millidarcys in the Guatemala Basin, a few degrees to the northwest of the Costa Rica Rift. Bryant et al. (1975), however, suggest that a more reasonable permeability for the entire sedimentary section is in the range of 10^{-4} to 0.1 millidarcys, and Crowe and Silva (1981) suggest values of up to 1 millidarcy for carbonaceous sediment at 200 meters depth. Thus, an average estimate for the permeability of the sediment column would seem to be about 0.1 millidarcy. However, the existence of chert over the lower 30 meters of sediment column (with permeability that is several orders of magnitude lower than that of the sediment) suggests very much lower values, and it seems reasonable to take 0.01 millidarcy as a maximum permeability for the sedimentary section. Taking $k_s = 0.01$

millidarcy, $h = 280$ m, $a = 6.3 \times 10^{-4} \text{m}^{-1}$, and $k_b = 4\text{--}40$ millidarcy, we have

$$\frac{k_s}{ahk_b} \ll 0.1 \quad (7)$$

Thus, the condition prescribed by Equation (1) is satisfied, and the low hydraulic admittance of the sediments apparently could seal a convection system.

To know whether the oceanic crust is convecting below such a seal, the $T > T_c$ requirement also must be met. The Rayleigh number of a porous medium convecting in response to a vertical temperature difference ΔT across a layer of thickness D is

$$R = \frac{k\alpha g \Delta T D}{\kappa_m \nu_m} \quad (8)$$

where α is the thermal expansion coefficient of the fluid, κ_m is the effective thermal diffusivity of the medium, and ν_w is the viscosity of sea water (Anderson and Skilbeck, in press).

Gartling (1981) shows that the optimum vertical transport in a convecting two-layered porous medium with properties of the oceanic crust and overlying sediment occurs when the aspect ratio is nearly unity. Given the theoretical heat flow for 6.1-m.y.-old sea floor and the observed mean heat flow (both at 200 mWm^{-2} ; Fig. 1B), the ΔT over a 3.0-km-thick convecting cell with 300 meters of impermeable sediments and an aspect ratio near unity would be $\sim 200^\circ\text{C}$. Then $R \approx 24$ to 240 if the bulk permeability of the convecting medium is ≈ 4 to 40 millidarcys. Because of the large thermal-expansion coefficient (Straus and Schubert, 1977) and the temperature-dependent viscosity of water (Kasoy and Zebib, 1975), R_c for the ocean crust is less than 10, whether the top of the cell is permeable or impermeable (Ribando et al., 1976). Therefore, convection in the basement is indicated strongly.

Further confirmation of convection in Layer 2 is seen in the negative pore pressure observed at the bottom of Hole 504B, if we could show that such a pressure drop could reasonably be generated in a porous-media convection cell. Gartling (1981) and Gartling and Anderson (in prep.) have constructed plane-layer finite-element models to examine convection in the oceanic crust and sedimentary layers. Though not exactly modelling the Costa Rica Rift case, a model with 220 mWm^{-2} of basal heat flow into a 3-km, two-layer porous media with aspect ratio of unity, $k_b = 10^{-10} \text{ cm}^2$, and $k_s = 10^{-13} \text{ cm}^2$ provides useful insight into the underpressure problem (Fig. 6). A plot of pressure in the cell (Fig. 6D) shows that a model with 100 meters of sediments predicts ~ 3 bar underpressures in the upper 500 meters of the oceanic crust. The pressure field shown in Figure 6D is appropriate for comparison with our measurements, because the values refer to the difference in pressure between the *in situ* pressure and the expected hydrostatic pressure for a column of fluid at a temperature of 1.5°C , which is essentially the condition introduced by the drill pipe and packer system.

The particular model shown in Figure 6 predicts lower bottom-hole temperatures (actual bottom-hole temperatures are about 120°C at 750 meters sub-sea-floor depth; Becker et al., this volume) and larger-amplitude variation in surface heat flow than actually observed (observed heat-flow variations are 175 to 275 mWm^{-2} ; Fig. 1). A model with 300 meters instead of 100 meters of impermeable sediments would increase the temperatures within the cell, while keeping the changes in temperature within the convection cell about the same. Thus, the sediment/basement interface temperature would increase substantially, and the amplitude of surface heat-flow variation would correspondingly decrease. Also, the predicted bottom-hole temperature for Hole 504B would increase into the appropriate range, and most important, the underpressures within the model would become even more negative. Thus, based upon the Gartling and Anderson (in prep.) modeling, the most logical explanation for observed underpressures in Hole 504B is active convection in the ocean crust beneath the sediments on the flank of the Costa Rica Rift.

CONCLUSIONS

We present here the first direct measurements of permeability and pore pressure in the oceanic crust. The relatively permeable nature of Layer 2A, especially compared to the overlying sedimentary lid with its basal chert layer, coupled with measurements of an underpressured zone beneath the sediment/basement contact, strongly indicates that DSDP Hole 504B penetrated a hydraulic lid into an active ocean crustal convection system several kilometers in extent. Just as the discovered "black smokers" were direct substantiation of the geophysical predictions of active convection at ridge axes, high permeability and underpressures, when coupled with other scientific findings of DSDP Leg 69 (particularly the thermal logs of Becker et al., this volume) represent substantiation of hypothesized convection on the flanks of mid-ocean ridges. It appears that Hole 504B penetrated into a high-permeability zone within a crustal convection cell. The hydraulic seal isolating this system from the oceanic bottom water apparently is so effective that pore pressures 2% less than hydrostatic can be sustained only 200 meters into the oceanic Layer 2A.

Much future work and many outstanding questions remain. What is the relative importance of the sediment layer, the chert layer, and the basaltic flows in affecting the hydraulic seal? How does permeability of these units vary with age on the flanks of mid-ocean ridges? How does permeability vary with depth in Layers 2 and 3 of the oceanic crust? On a smaller scale, how does the pore pressure vary across the proposed convection cell near Hole 504B? Where does the water drawn into the oceanic crustal aquifer at Hole 504B go? Does it reappear at the sea floor somewhere nearby, or will it ever reappear? For how long will the system continue to draw water into the oceanic crust? Questions such as these will be answered only by further down-hole experimentation at this and other sites, on drilling ships such as the *D/V Glomar Challenger*.

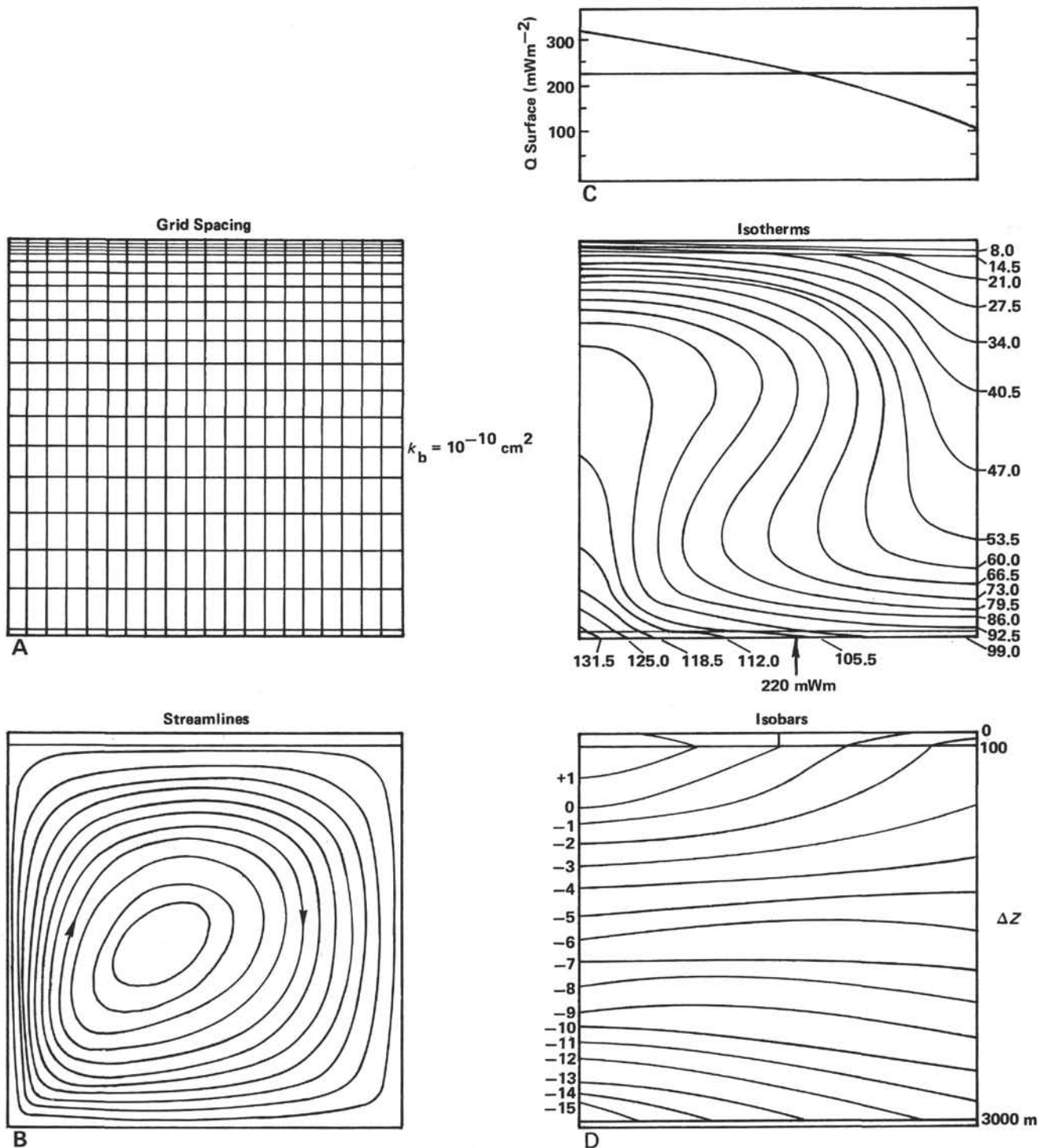


Figure 6. A finite-element model of Hole 504B geometry from Gartling and Anderson (in prep.). Sediment permeability is 0.01 millidarcys and basalt permeability is 10 millidarcys. The lateral boundaries of the domain are assumed to be adiabatic and impermeable. The sediment surface is maintained at a constant temperature and pressure of 1.5°C and 600 bars, respectively. The lower boundary is impermeable, with an imposed heat flux of 220 mWm^{-2} . Material properties include variable viscosity, thermal conductivity, and thermal-expansion coefficient. The fluid is Boussinesq. The pressure plot (D) is presented as the *in situ* pressure minus the hydrostatic pressure appropriate to a column of fluid at 1.5°C .

ACKNOWLEDGMENTS

We wish to thank the officers and crew of the D/V *Glomar Challenger*, particularly the Global Marine roughnecks, for efforts expended on behalf of these experiments. Glen Foss, the Operations Manager, Otis Winton, the Drilling Superintendent, and Joe Svitek of the USGS were major contributors to the success of these experiments. The manuscript benefited greatly from review by C. B. Raleigh, J. Bredehoeft, and S. Hickman. This work was supported by National Science Foundation grant OCE-78-27026.

REFERENCES

- Abbott, D. W., Menke, M., Hobart, M. A., and Anderson, R. N., in press. Evidence of excess pore pressures in southwest Indian Ocean sediments. *J. Geophys. Res.*
- Anderson, R. N., and Hobart, M. A., 1976. The relation between heat flow, sediment thickness and age in the eastern Pacific. *J. Geophys. Res.*, 77:4472-4475.
- Anderson, R. N., Hobart, M. A., and Langseth, M. G., 1979. Geothermal convection through the oceanic crust and sediments in the Indian Ocean. *Science*, 204:828-832.
- Anderson, R. N., Langseth, M. G., and Sclater, J. G., 1977. The mechanisms of heat transfer through the floor of the Indian Ocean. *J. Geophys. Res.*, 82:3391-3409.
- Anderson, R. N., and Skilbeck, J. N., in press. Oceanic heat flow. In Emiliani, C. (Ed.), *The Sea* (Vol. 7): New York (Wiley-Interscience).
- Anderson, R. N., and Zoback, M., in press. The implications of fracture distribution, structure, and stratigraphy from borehole televiewer imagery of the oceanic crust on the Costa Rica Rift. *J. Geophys. Res.*
- Bredehoeft, J. D., and Papadopoulos, S. S., 1980. A method for determining the hydraulic properties of tight formations. *Water Resources Res.*, 16:233-238.
- Bryant, W. R., Hottman, W., and Trabant, P. T., 1975. Permeability of unconsolidated and consolidated marine sediments, Gulf of Mexico. *Mar. Geotech.*, 1:1-13.
- Clark, W. B., Beg, M. A., and Craig, H., 1970. Excess He in the sea: evidence for terrestrial primordial helium. *Earth Planet. Sci. Lett.*, 9:45.
- Cooper, H. H., Bredehoeft, J. D., and Papadopoulos, S. S., 1967. Response of a finite-diameter well to an instantaneous charge of water. *Water Resources Res.*, 3:263-269.
- Corliss, J., et al., 1979. Submarine thermal springs on the Galapagos Rift. *Science*, 203:1973.
- Crowe, J., and Silva, A., in press. Permeability measurement of equatorial Pacific carbonate ooze using direct measurement back-pressure techniques. *J. Geophys. Res.*
- CRRUST, in press. Drilling results from IPOD legs 69 and 70, Site 504B on the Costa Rica Rift. *Geol. Soc. Am. Bull.*
- Davis, E. E., Lister, C. R., Wade, U. S., and Hyndman, R. D., 1980. Detailed heat flow measurements over the Juan de Fuca Ridge System. *J. Geophys. Res.*, 81:299,310.
- Edmond, J., et al., 1979. Ridge crest hydrothermal activity and the balances of the major and minor elements in the ocean: the Galapagos data. *Earth Planet. Sci. Lett.*, 46:1-12.
- Ferris, J. G., and Knowles, D. B., 1954. The slug test for estimating transmissibility. *U.S. Geol. Surv. Ground Water Note 26.*
- Gartling, D. K., 1981. Finite element analysis of thermal convection in deep ocean sediments. *Proceedings Third International Conference on Finite Elements: Water Resources Res.*, 1981.
- Gartling, D. K., and Anderson, R. N., in prep. Finite element model of two layer porous media convection in the oceanic crust and overlying sediments.
- Green, K. E., Von Hursen, R. P., and Williams, D. L., 1981. The Galapagos Spreading Center at 86°W, a detailed geothermal field study. *J. Geophys. Res.*, 86:979,986.
- Johnson, D. M., 1980b. Fluid permeability of oceanic basalts. In Robinson, P., Flower, M., Salisbury, M., et al., *Init. Repts. DSDP*, 51, 52, 53, Pt. 2: Washington (U.S. Govt. Printing Office), 1473-1477.
- Kassoy, D. R., and Zebib, Z., 1975. Variable viscosity effects on the onset of convection in porous media. *Phys. Fluids*, 18:1649-1651.
- Lister, C. R., 1972. On the thermal balance of Ridges. *Geophys. J. Royal Astron. Soc.*, 26:515-530.
- Lupton, J. E., Klinkhammer, G. P., Normark, W. R., Haymon, R., Macdonald, K. C., Weiss, R. F., and Craig, H., 1980. Helium-3 and manganese at 21°N East Pacific Rise hydrothermal site. *Earth Planet. Sci. Lett.*, 50 (No. 2):115-127.
- Matthews, C. S., and Russell, D. G., 1967. Pressure build-up and flow tests in wells. *Soc. Petrol. Eng. Monogr.*, Vol. 1.
- Ribando, R. J., Torrence, K. E., and Turcotte, D. L., 1976. Numerical models for hydrothermal circulation in the oceanic crust. *J. Geophys. Res.*, 81:3007-3012.
- Salisbury, M. H., et al., 1979. The physical state of the upper levels of Cretaceous oceanic crust from the results of logging, laboratory studies and the oblique seismic experiment at DSDP Sites 417 and 418. In Talwani, M., Harrison, C., and Hayes, D. (Eds.), *Deep Drilling Results in the Atlantic Ocean: Ocean Crust*: Washington (Am. Geophys. Union), pp. 113-134.
- Sclater, J. G., Crowe, J., and Anderson, R. N., 1976. On the reliability of oceanic flow averages. *J. Geophys. Res.*, 81:2997-3006.
- Snow, D. T., 1968. Rock fracture spacing, openings and porosities. *J. Soil Mech. Foundation Div., ASCE Proc.*, 94.
- Spiess, F. N., et al., 1980. Geothermal system at 21°N: East Pacific Rise, geophysical observations. *Science*, 207:1421-1432.
- Williams, D. L., Von Herzen, R. P., Sclater, J. G., and Anderson, R. N., 1974. The Galapagos spreading center: lithospheric cooling and hydrothermal circulation. *Geophys. J. Royal Astron. Soc.*, 38:587.
- Zemanek, J., Caldwell, R. C., Glenn, E. E., Jr., and Norton, L. J., 1970. Formation evaluation by inspection with the borehole televiewer. *Geophysic.*, 35 (No. 2):254-269.